The EMBO Journal Vol.17 No.10 pp.2748–2758, 1998

Nine hydrophobic side chains are key determinants of the thermodynamic stability and oligomerization status of tumour suppressor p53 tetramerization domain

Mauricio G.Mateu[1] and Alan R.Fersht[2]

Cambridge University Chemical Laboratory and Cambridge Centre for Protein Engineering, MRC Centre, Hills Road, Cambridge CB2 2QH, UK

[1]On leave from Universidad Autónoma de Madrid, Spain

[2]Corresponding author
e-mail: arf10@cam.ac.uk

The contribution of almost each amino acid side chain to the thermodynamic stability of the tetramerization domain (residues 326–353) of human p53 has been quantitated using 25 mutants with single-residue truncations to alanine (or glycine). Truncation of either Leu344 or Leu348 buried at the tetramer interface, but not of any other residue, led to the formation of dimers of moderate stability (8–9 kcal/mol of dimer) instead of tetramers. One-third of the substitutions were moderately destabilizing (<3.9 kcal/mol of tetramer). Truncations of Arg333, Asn345 or Glu349 involved in intermonomer hydrogen bonds, Ala347 at the tetramer interface or Thr329 were more destabilizing (4.1–5.7 kcal/mol). Strongly destabilizing (8.8–11.7 kcal/mol) substitutions included those of Met340 at the tetramer interface and Phe328, Arg337 and Phe338 involved peripherally in the hydrophobic core. Truncation of any of the three residues involved centrally in the hydrophobic core of each primary dimer either prevented folding (Ile332) or allowed folding only at high protein concentration or low temperature (Leu330 and Phe341). Nine hydrophobic residues per monomer constitute critical determinants for the stability and oligomerization status of this p53 domain.
Keywords: alanine-scan mutagenesis/oligomerization/p53/protein stability and folding

Introduction

Human protein p53 is a homotetrameric, multifunctional transcription factor which acts as a natural tumour suppressor (reviewed in Picksley and Lane, 1994; Arrowsmith and Morin, 1996; Ko and Prives, 1996; Levine, 1997). Each p53 monomer (393 amino acids) consists of at least five functional regions: an N-terminal transactivation region, a DNA-binding core domain, a nuclear localization signal, a tetramerization (tet) domain and a C-terminal regulatory region. Both DNA binding and tetramerization have been proven essential for efficient p53 function. However, the majority of the many p53 mutations associated with cancer are found in the core domain while <1% involve the tet domain (Hollstein *et al.*, 1991, 1996). To explain this biased distribution in tumour cells, two proposals have been advanced (comments in Hann and Lane, 1995; Arrowsmith and Morin, 1996): (i) mutations in the p53 tet domain are not selected for because most single amino acid changes are unable to destabilize the tetramer enough to prevent p53 oligomerization and function (Jeffrey *et al.*, 1995); and (ii) mutations in p53tet are selected against because of a functional role of this domain in cell transformation. This latter hypothesis is based on observations of a dominant-negative effect of mutant p53 (with an intact tet domain) in tumour suppression (e.g. Harvey *et al.*, 1995), and of the transdominant transforming activity of a p53 fragment which contained the non-mutated tetramerization domain (Shaulian *et al.*, 1992). These results led to the proposal that defective p53 with an intact tet domain would be able to sequester non-mutated p53 through the formation of inactive hetero-oligomers.

The implications of the above observations for the development of anticancer gene therapy based on p53 (Beaudry *et al.*, 1996) have stimulated structure–function studies of p53tet. This domain has been mapped by using proteolytic fragments and deletion mutants and peptides (Shaulian *et al.*, 1992; Stürzbecher *et al.*, 1992; Pavletich *et al.*, 1993; Sakamoto *et al.*, 1994; Wang *et al.*, 1994), and its three-dimensional structure determined by both X-ray crystallography (Jeffrey *et al.*, 1995; Miller *et al.*, 1996) and NMR spectroscopy (Clore *et al.*, 1994, 1995; Lee *et al.*, 1994). Each monomer is comprised of a β-strand (p53 residues 326–333), a tight turn (Gly334) and an α-helix (residues 335–353 or 355). The tetramer can be described as a dimer of dimers, with each primary dimer formed by an antiparallel β-sheet and two antiparallel α-helices, and the two dimers arranged in a roughly orthogonal way forming an unusual four-helix bundle (Figure 1). A quantitative analysis of the thermodynamic stability of non-mutated, isolated p53tet showed that its thermal denaturation can be described as a reversible, two-state transition in which the folded tetramer is converted directly to denatured monomers (Johnson *et al.*, 1995). Qualitative insights into the contribution of some amino acid residues within the tet domain to oligomerization, DNA binding or biological functions of p53 have been gained by introducing a number of single and multiple mutations in the full-length protein (Stürzbecher *et al.*, 1992; Ishioka *et al.*, 1995; Waterman *et al.*, 1995; Chène *et al.*, 1997; McCoy *et al.*, 1997). Some full-length p53 mutants substituted at position 344 bound DNA as dimers instead of tetramers, and a triply mutated, isolated tet was found to be a dimer with an altered tertiary structure (McCoy *et al.*, 1997).

Here we describe the truncation of almost each amino acid side chain within p53tet by mutation to alanine, and the evaluation of the effect of each single substitution on the thermodynamic stability and the oligomerization status of the isolated p53tet. The strength of the alanine-scan

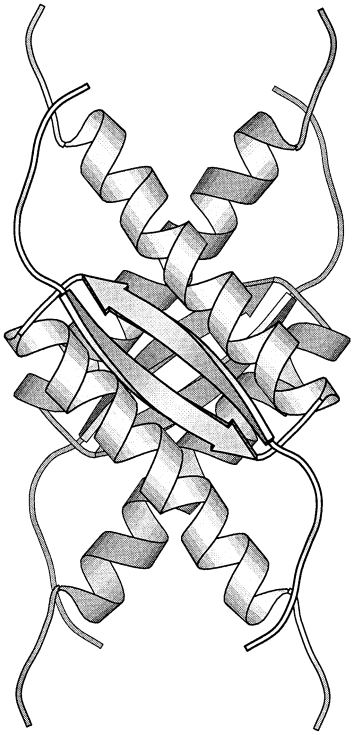

Fig. 1. Ribbon model of the p53tet structure. The program Molscript (Kraulis, 1991) and the p53tet (residues 319–360) coordinates deposited in the Brookhaven Protein Data Bank (1sak; Clore *et al.*, 1995) were used. The two primary dimers are shown in light and dark shades of grey, respectively. The N- and C-terminal tails represented are disordered in the different structures determined by NMR and X-ray crystallography.

approach is that it allows an unbiased quantitative analysis of the specific contribution of each side chain to protein stability (Milla *et al.*, 1994; Yu *et al.*, 1995). The results presented provide new insights into the stability, folding and oligomerization of p53tet and of oligomeric proteins in general, and constitute a basis for the rational design of a variant tet domain useful in the development of p53 gene therapy.

Results

Thermodynamic stability and delimitation of the p53 tetramerization domain

The version used by Johnson *et al.* (1995) for their thermal denaturation analysis of non-mutated p53tet (tetL; p53 residues 303–366; Figure 2) contained the structurally defined domain, flanked by 11-residue C-terminal tails and 25-residue N-terminal tails which included most of the p53 segment connecting tet with the DNA-binding domain. We have constructed tetL and three shorter versions, tetS, tet SS and tetP (the latter corresponding exactly to the structurally defined domain; Figure 2). Size-exclusion chromatography analysis (at ~100 μM tetramer) showed tetL, tetS and tetSS to be in their tetrameric form with no traces of free monomer. Comparison of the far UV–circular dichroism (CD) spectra of the three versions suggested that the p53 segment 303–318 which links tet with the core domain could be essentially unstructured (data not shown). The synthetic tetP was also folded and tetrameric as indicated by CD and analytical size-exclusion chromatography (see below).

Changes in the fluorescence spectra of p53tet upon denaturation were too small to monitor unfolding accurately, as expected from the absence of tryptophans and the high solvent exposure of the only tyrosine present. Instead, CD spectroscopy was used. The thermodynamic data obtained from chemical and thermal denaturation analysis of wild-type p53tet are summarized in Table I. Two-state transition analysis yielded the same thermodynamic values on guanidinium hydrochloride (GuHCl) denaturation of tetS or on renaturation of denatured tetS (Figure 3A). Very similar values for the free energy of unfolding extrapolated to absence of denaturant, $\Delta G_u^{H_2O}$ were also obtained using different tetS concentrations and either urea or GuHCl as denaturant (Figure 3B). The concentration of denaturant at which the transition is half-completed, $[D]_{50\%}$, was dependent on the protein concentration in the way expected for a coupled unfolding–dissociation process from native tetramers to denatured monomers (see Materials and methods). Thus, chemical denaturation of p53tet can be described as a completely reversible two-state transition. As expected from the results obtained for tetL by Johnson *et al.* (1995), thermal denaturation of the shorter tet versions followed by CD—and for tetS also by differential scanning calorimetry (DSC)—appeared also as a completely reversible two-state process (Table I and data not shown).

The four versions of p53tet yielded similar values for each thermodynamic parameter (Table I). For tetSS, $\Delta G_u^{H_2O}$ = 32.4 kcal/mol of tetramer (at 25°C and a 1 M standard state concentration) and T_m = 75.2°C (at 10 μM protein monomer concentration). Lengthening to tetS had very low or no effect on stability, while lengthening to tetL decreased $\Delta G_u^{H_2O}$ by ~0.7 kcal/mol of tetramer and T_m by 2.9°C. Shortening of tetSS to tet P decreased $\Delta G_u^{H_2O}$ by 1.4 kcal/mol of tetramer and T_m by 5.7°C (Table I). There is some inherent error in the calculation of $\Delta G_u^{H_2O}$ because of the errors in *m*-values (the variation in ΔG_u with the denaturant concentration) and the lengthy extrapolation of experimental ΔG_u values to absence of denaturant (Jackson *et al.*, 1993). Thus, the differences in stability, $\Delta\Delta G_u$ were more accurately quantitated at a denaturant concentration intermediate between the $[D]_{50\%}$ of any two variants, and given as $\Delta\Delta G_u^{[D]_{50\%}}$ (see Materials and methods). The $\Delta\Delta G_u^{[D]_{50\%}}$ values for tetL and tetP relative to tetSS were 0.9 kcal/mol of tetramer and 0.5 kcal/mol of tetramer respectively, which confirmed the slightly higher stability of tetSS and tetS.

Contribution of each amino acid side chain to the thermodynamic stability and oligomerization of the p53 tetramerization domain

Site-directed mutagenesis of tetS was used to construct a systematic set of mutants with a single alanine substitution per monomer. All but one of the 25 non-alanine, non-glycine residues in each of the monomeric segments that structurally define the tetramerization domain (p53 positions 326–353, Figures 1 and 2) were substituted. The exception was the solvent-exposed Tyr327, used as a reporter to determine protein concentration. Truncation of Ala347 to Gly was also tested. TetS was chosen as the reference protein instead of tetSS because the former was found to be expressed to a substantially higher level. High-level expression and purification was achieved for

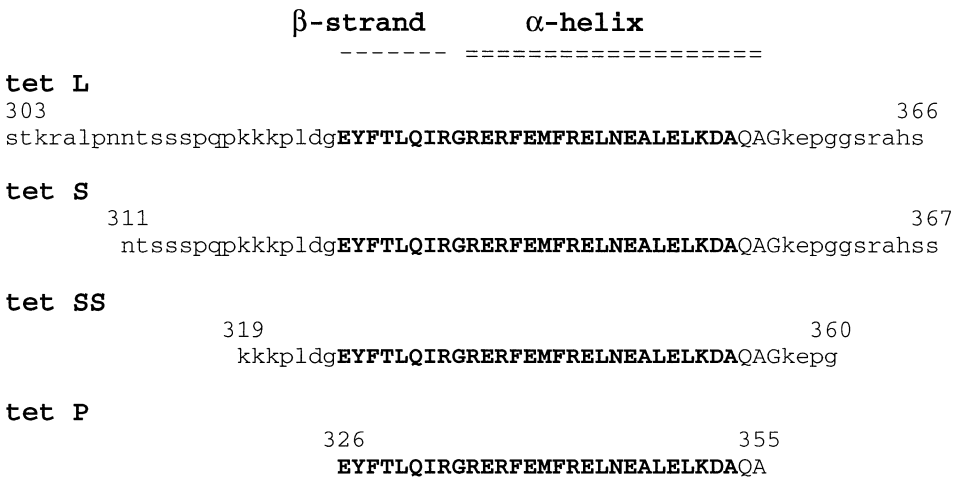

Fig. 2. Four versions of human p53tet analysed. TetL, tetS and tetSS were obtained as recombinant polypeptides and correspond to the p53 fragments prepared by Lee *et al.* (1994), Jeffrey *et al.* (1995), Clore *et al.* (1994, 1995) and Miller *et al.* (1996) for their structural analyses. TetP was obtained as a synthetic peptide (see Materials and methods). The residues found ordered in all of these structural studies are shown in boldface.

Table I. Thermodynamic parameters[a] for wild-type p53tet

p53tet	*m* [kcal/(M.mol)]	$[D]_{50\%}$ (M)	$\Delta\Delta G_u^{H_2O}$ (kcal/mol)	$\Delta G_u^{[D]50\%}$ (kcal/mol)	T_m (°C)	ΔH_u^{Tm} (kcal/mol)
TetL	5.0±0.3	2.64±0.03	31.7±0.9	0.9±0.2	72.3±0.05	162±1.2
TetS	5.1±0.2	2.78±0.01	32.5±0.5	0.2±0.1	73.5±0.03	165±0.9
TetSS	4.9±0.1	2.82±0.01	32.4±0.4		75.2±0.02	164±0.7
TetP	4.6±0.2	2.73±0.02	30.9±0.5	0.5±0.1	69.5±0.03	155±0.9

[a]*m*, variation in the free energy of unfolding, ΔG_u, with the GuHCl concentration; $[D]_{50\%}$, concentration of GuHCl at which the transition is half-completed, using 40 μM protein (monomer) concentration. $\Delta G_u^{H_2O}$, ΔG_u extrapolated to absence of denaturant; $\Delta\Delta G^{[D]50\%}$, difference in ΔG_u between tetSS and any variant at a GuHCl concentration intermediate between the $[D]_{50\%}$ of the two proteins; T_m, transition temperature; ΔH_u^{Tm}, variation in the enthalpy of unfolding at the transition temperature. The standard errors of fitting are indicated.

22 mutants. Electrospray mass spectrometry analysis of a representative subset of the mutants gave the expected molecular mass (±1 Da) in each case, which further confirmed the sequencing and electrophoresis results. Analytical gel filtration of all mutants (at an initial concentration of 40 μM monomer, the same used in the GuHCl denaturation assays) showed that most of these mutants were tetramers with exactly the same K_{av} as wild-type tetS (K_{av} = 0.20) or, in the case of Met340 and especially Arg337, somewhat higher. In contrast, mutants Leu344Ala and Leu348Ala migrated as dimers (K_{av} = 0.31) (Figure 4). These values are substantially lower than expected for globular proteins of the same length, but are in perfect agreement with the results obtained by McCoy *et al.* (1997) for the native tetramer and a dimeric triple mutant of another version of p53tet.

Mutants substituted at Leu330, Ile332 or Phe341 were detected only in minor amounts in the cellular extracts. Changes in bacterial strain or experimental conditions did not improve the expression levels, and these three variants were obtained instead as synthetic peptides homologous to tetP. Comparison with tetP by CD spectroscopy and gel filtration (Figure 5) indicated that the three mutants were essentially unfolded at 25°C and 10 μM monomer concentration. However, mutants Leu330Ala and Phe341Ala were quantitatively folded at higher protein concentrations and lower temperatures (Figure 5A). The mutant Ile332Ala was unfolded and monomeric even at the lowest temperatures and highest protein concentrations tested (Figure 5A and data not shown).

The set of p53tet mutants obtained was analysed by GuHCl and thermal denaturation experiments. Some representative results are shown in Figure 6. The values determined for the relevant thermodynamic parameters are summarized in Table II and, except for the dimeric mutants Leu344Ala and Leu348Ala, refer to the unfolding of tetramer and were compared with those of the parental tetS. Because each single mutation affected four identical side chains (one in each monomer) the $\Delta\Delta G_u$ values obtained should be divided by four to obtain the contribution of each individual side chain tested. GuHCl denaturation analysis showed that truncation to Ala of any residue, except the solvent-exposed Glu336 and Glu343, had a substantial effect on the stability of p53tet ($\Delta\Delta G_u^{[D]_{50\%}}$ >1.6 kcal/mol of tetramer). Truncation of the partially buried Lys351 appeared to have some stabilizing effect (see below). Moderately destabilizing (1.6–3.9 kcal/mol) mutations affected most residues highly accessible to solvent, including Gln331 and many charged amino acids (Glu326, Glu339, Glu346, Asp352, Arg335 and Arg342), and the partially accessible Leu350. Truncations of the solvent-accessible Thr329, a triad of amino acids involved in two clusters of intermonomer hydrogen bonds in each primary dimer (Arg333, Asn345, Glu349) or the buried Ala347 were more substantially destabilizing (4.1–5.7 kcal/mol). Truncation of the hydrophobic core residues

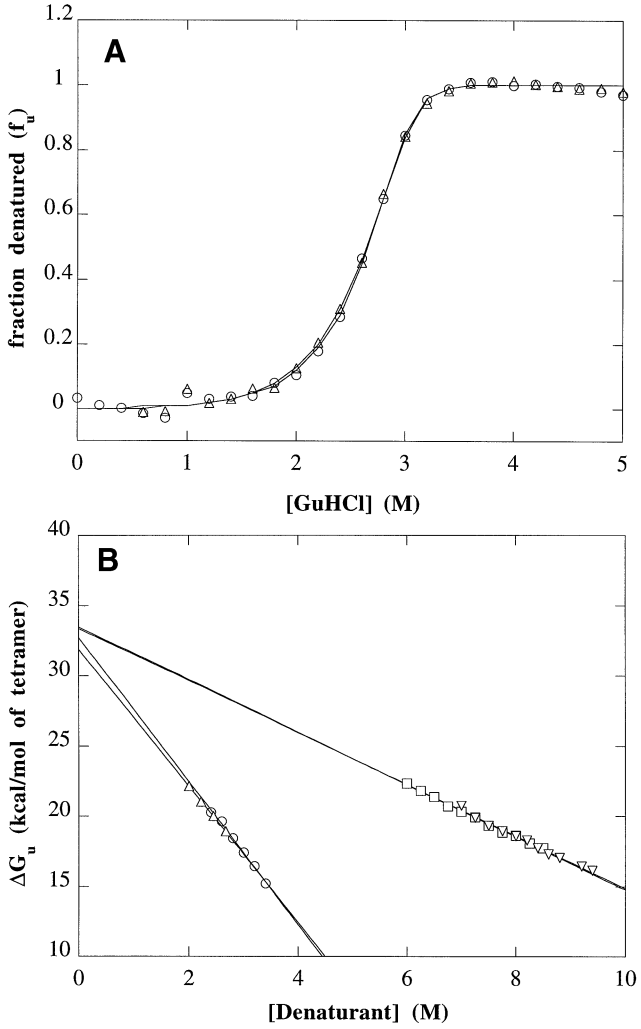

Fig. 3. (**A**) Reversible GuHCl denaturation of p53tetS. The fraction of protein denatured at 25°C is represented as a function of the final GuHCl concentration, both for denaturation of native protein (○) and for renaturation of previously denatured protein (△). The protein concentration was 40 μM monomer. The fitting of the experimental f_u values to two-state transition curves (folded tetramer-denatured monomer) using the program Excel (see Materials and methods) is indicated by solid lines. (**B**) Extrapolation to absence of denaturant of ΔG_u values obtained for p53tetS at 21°C in GuHCl denaturation experiments at 40 μM (○) or 8 μM (△) monomer concentration, or in urea denaturation experiments at 40 μM (▽) or 8 μM (□) monomer concentration. Linear fitting of the experimental ΔG_u values obtained is indicated by the solid lines.

Phe328, Arg337, Phe338 or Met340 strongly destabilized (8.8–11.7 kcal/mol) p53tet. Finally, the destabilization caused by truncation of any of the hydrophobic core residues Leu330, Ile332 and Phe341 prevented folding at the reference temperature and protein concentration used.

Thermal denaturation analysis of the same set of mutants (Table II) essentially confirmed the results obtained by chemical denaturation. At 10 μM monomer concentration all mutants except Ile332Ala showed a completely reversible cooperative transition with a T_m which ranged from 78.6°C (Glu336Ala) to <15°C (Leu330Ala and Phe341Ala). For these two latter mutants only a part of the transition curve could be observed and the thermodynamic parameters could not be determined. However, the use of a higher protein concentration (280 μM monomer) allowed

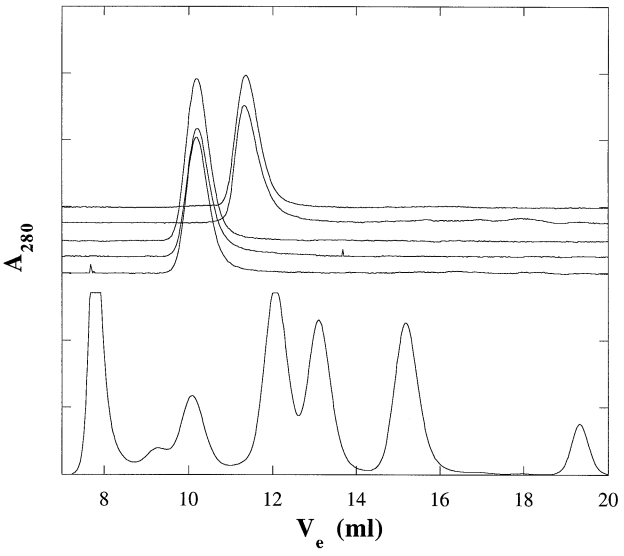

Fig. 4. Analytical size-exclusion chromatography of wild-type p53tetS and some representative mutants. The experiments were carried out as described in Materials and methods. The column was calibrated using a set of molecular weight markers as shown on the lower part of the figure. The peaks correspond to thyroglobulin (660 kDa, V_0), bovine serum albumin (67 kDa), ovalbumin (43 kDa), chymotrypsin (25 kDa), ribonuclease A (13.7 kDa), aprotinin (6.5 kDa) and acetone (V_t). p53tet chromatograms are shown on the upper part and have been offset for clarity. They correspond (from bottom to top) to Glu336Ala, Phe338Ala, wild-type tetS, Leu348Ala and Leu344Ala. The initial (monomer) concentration was 40 μM.

the destabilization caused by truncation of Leu330 to be estimated; $\Delta\Delta G_u$ values calculated at the T_m of wild-type tetS or at 25°C were $\Delta\Delta G_u^{T_m} = 22$ kcal/mol and $\Delta\Delta G_u^{25°C} = 19$ kcal/mol, respectively. Phe341Ala at high protein concentrations aggregated when heated. Ile332Ala was denatured even at low temperature and did not show any cooperative transition on heating from 2°C. For the other mutants a good linear correlation was found between $\Delta H_u^{T_m}$ and T_m ($r = 0.95$). The $\Delta\Delta G_u^{T_m}$ values (Table II) cannot be very accurate, however, partly because of the limited temperature interval at which denaturation occurs and of wide differences in T_m, and also because not all the relevant parameters can be determined in the absence of DSC analysis (Johnson *et al.*, 1997). In addition, the difference in stability between any two proteins may depend on the temperature or denaturant concentration at which it is measured. A few significant discrepancies were indeed found, including the truncation of Lys351 which was moderately stabilizing in GuHCl ($\Delta\Delta G_u^{[D]_{50\%}} = -2.1$ kcal/mol) but somewhat destabilizing at high temperatures ($\Delta T_m = 5$°C). In spite of these exceptions, a good linear correlation ($r = 0.89$) between $\Delta\Delta G_u^{[D]_{50\%}}$ and $\Delta\Delta G_u^{T_m}$ was observed, with a slope close to 1 (1.04 ± 0.13).

Thermodynamic stability of dimeric variants of the p53 tetramerization domain

The stability of the dimeric forms of the p53 oligomerization domain obtained by truncation to Ala of Leu344 or Leu348 was also quantitated (Figure 7 and Table II). As for tetrameric p53tet, denaturation was completely reversible and could be fitted to two-state transition curves. The analyses of Leu344Ala and Leu348Ala yielded

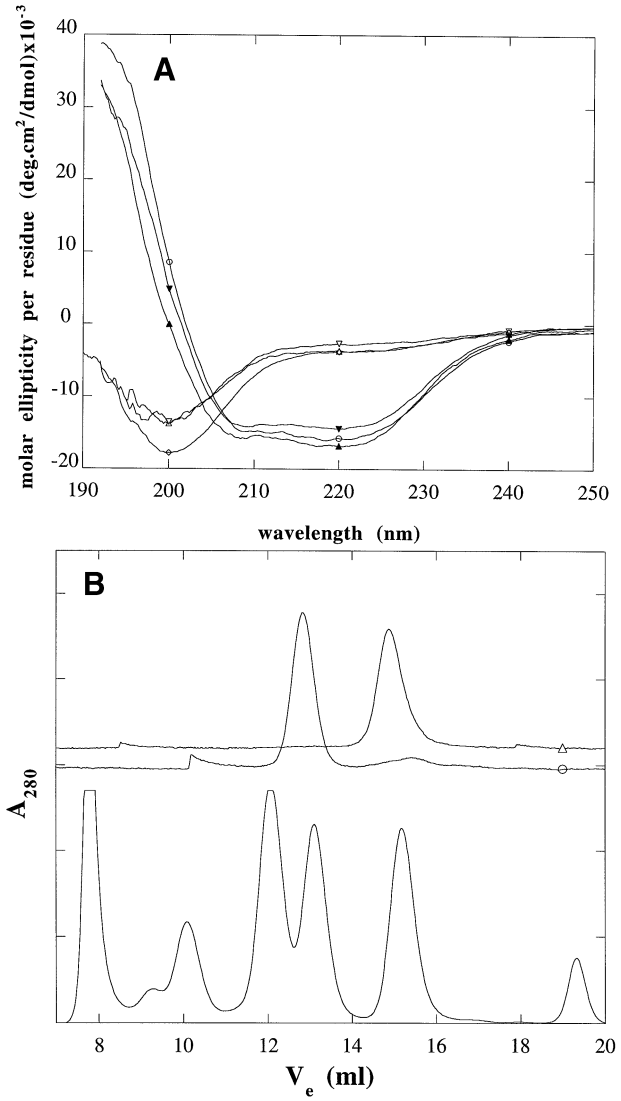

Fig. 5. (**A**) CD spectra of p53tetP and mutants. ○, 40 μM wild-type tetP at 25°C; △, 10 μM Phe341Ala at 25°C; ▲, 336 μM Phe341Ala at 5°C; ▽, 10 μM Leu330Ala at 25°C; ▼, 280 μM Leu330Ala at 4°C; ◇, 328 μM Ile332Ala at 2°C (all concentrations referred to monomer). The ellipticity values have been normalized. (**B**) Analytical size-exclusion chromatography of wild-type tetP and mutant Phe341Ala. Molecular weight markers (lower part) are those described in Figure 4. p53tet chromatograms (upper part) have been offset for clarity and correspond to wild-type tetP (○) and Phe341Ala (△), both at 40 μM initial (monomer) concentration.

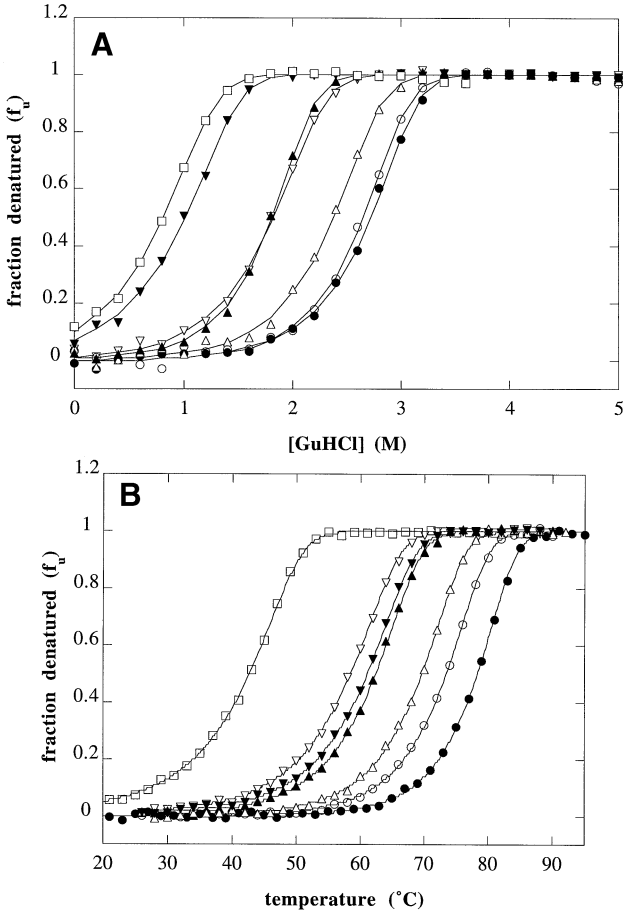

Fig. 6. GuHCl denaturation at 25°C (**A**) and thermal denaturation (**B**) of p53tetS and some representative tetrameric mutants. The fraction of protein denatured is represented as a function of GuHCl concentration or temperature for wild-type tet S (○) and mutants Glu336Ala (●), Glu346Ala (△), Ala347Gly (▲), Arg333Ala (▽), Phe338Ala (▼), Arg337Ala [□ in (A)] and Phe328Ala [□ in (B)]. The protein (monomer) concentration was 40 μM in (A) or 10 μM in (B). The fitting of the experimental values to two-state transition curves using the program Excel is indicated by solid lines. For clarity, only one in every 10 experimental points is represented in (B).

$\Delta\Delta G_u^{H_2O}$ = 9.3 kcal/mol of dimer and 8.2 kcal/mol of dimer, respectively (at 25°C and a 1 M standard state concentration) and T_m = 46.9°C and 42.2°C at 10 μM protein (monomer) concentration.

Discussion

The p53 linker region appears essentially unstructured

Structural studies of p53tet revealed a compact domain (residues 326–353 or 355) flanked by disordered peptide tails. However, it has been suggested that some residual structure could be present in these disordered segments (Johnson *et al.*, 1995). We observed that extension of the structurally defined domain by five to seven residues at both ends did stabilize the protein but only by a small amount. Further N-terminal extensions had either no effect (segment 311–318) or caused a small decrease in stability of ~1 kcal/mol (segment 303–318). The longer extension was shown previously to diminish by 1.3 kcal/mol the free energy of dissociation ΔG_D of p53tet (Sakamoto *et al.*, 1994). It thus appears that the p53 segment 303–310 has a minor negative effect on the intrinsic stability of the tet domain proper. Some effect of the phosphorylation of p53 residues located outside tet on ΔG_D has been described (Sakaguchi *et al.*, 1997), which also suggests some interaction of tet with other p53 segments. The above observations, however, allow the tetramerization domain to be essentially delimited between residues 326–355, both structurally and thermodynamically. They also indicate that most of the p53 linker region connecting the DNA-binding and tetramerization domains may be unstructured. Flexibility of this region may be necessary for p53 function (El-Deiry *et al.*, 1992; Pavletich *et al.*, 1993; Jeffrey *et al.*, 1995).

Table II. Thermodynamic parameters[a] for mutant p53tet

Mutant	*m* [kcal/(M.mol)]	$[D]_{50\%}$ (M)	$\Delta G_u^{H_2O}$ (kcal/mol)	$\Delta\Delta G_u^{H_2O}$ (kcal/mol)	$\Delta\Delta G_u^{[D]50\%}$ (kcal/mol)	T_m (°C)	ΔH_u^{Tm} (kcal/mol)	$\Delta\Delta G_u^{Tm}$ (kcal/mol)	S-ch. access (%)[b]
wt tetS	5.1±0.2	2.78±0.01	32.5±0.5			73.5±0.03	165±0.9		
E326A	5.0±0.3	2.48±0.02	30.9±0.7	1.6±0.8	1.6±0.1	70.2±0.03	161±0.8	1.6	92
F328A	10.5±0.6	0.64±0.01	25.3±0.4	7.2±0.7	11.7±0.2	43.4±0.03	112±0.5	13.0	46
T329A	5.4±0.3	1.93±0.02	28.8±0.5	3.6±0.7	4.6±0.2	67.1±0.04	162±1.0	3.2	101
L330A unfolded									22
Q331A	5.3±0.4	2.37±0.03	31.0±0.9	1.4±1.0	2.3±0.2	71.6±0.03	161±0.7	0.9	79
I332A unfolded									0
R333A	5.2±0.4	1.96±0.03	28.5±0.8	3.9±0.9	4.5±0.2	59.8±0.04	145±0.9	6.5	70
R335A	5.8±0.2	2.07±0.01	30.3±0.5	2.1±0.7	3.9±0.1	63.7±0.03	148±0.7	4.6	94
E336A	6.1±0.3	2.81±0.02	35.5±0.8	–3.0±0.9	–0.14±0.1	78.6±0.03	179±0.9	–2.5	102
R337A	5.0±0.4	0.94±0.03	23.1±0.4	9.3±0.6	10.0±0.3	34.3±0.08	79±0.6	14.1	53
F338A	6.0±0.2	1.13±0.01	25.2±0.2	7.2±0.6	9.0±0.2	53.2±0.02	115±0.5	8.2	36
E339A	5.7±0.3	2.14±0.02	30.6±0.7	1.8±0.8	3.5±0.2	70.5±0.03	175±1.2	1.6	84
M340A	6.5±0.5	1.17±0.02	26.1±0.5	6.4±0.7	8.8±0.2	54.6±0.05	129±1.0	8.4	41
F341A unfolded									0
R342A	5.1±0.3	2.49±0.02	31.0±0.7	1.4±0.8	1.6±0.2	66.0±0.03	154±0.7	3.6	69
E343A	5.0±0.07	2.62±0.005	31.4±0.2	1.1±0.5	0.9±0.1	73.8±0.03	161±0.7	–0.13	73
L344A dimer	3.0±0.1	1.11±0.01	9.3±0.2			46.9±0.03	70±0.3		0
N345A	5.1±0.2	2.02±0.02	28.7±0.5	3.7±0.7	4.1±0.2	69.5±0.04	148±1.0	1.8	18
E346A	5.5±0.3	2.47±0.02	32.1±0.7	0.4±0.9	1.7±0.1	70.1±0.04	164±0.9	1.7	79
A347G	6.1±0.3	1.87±0.02	29.8±0.7	2.7±0.8	5.0±0.2	63.2±0.04	151±0.9	4.9	0
L348A dimer	2.7±0.07	0.82±0.01	8.2±0.1			42.2±0.02	58±0.2		14
E349A	5.9±0.1	1.73±0.01	28.7±0.2	3.8±0.6	5.7±0.2	61.3±0.03	137±0.8	5.4	74
L350A	4.9±0.2	2.43±0.02	30.4±0.5	2.1±0.7	1.9±0.2	67.7±0.03	159±0.7	2.8	43
K351A	5.2±0.3	3.17±0.03	34.9±0.9	–2.5±1	–2.1±0.2	68.5±0.05	171±1.3	2.6	65
D352A	5.2±0.2	2.28±0.02	30.3±0.5	2.2±0.7	2.7±0.1	66.7±0.02	140±0.5	2.9	83

[a]The thermodynamic parameters are as defined in Table I. In addition, $\Delta\Delta G_u^{H_2O}$ is the difference in ΔG_u between wild-type tet S and any mutant at zero denaturant concentration; $\Delta\Delta G_u^{H_2O}$ values are less accurate than $\Delta\Delta G_u^{[D]50\%}$ because of the long extrapolation of experimental ΔG_u values to absence of denaturant. The standard errors of fitting are indicated. $\Delta\Delta G_u^{Tm}$ is the difference in ΔG_u between wild-type tetS and any mutant at the transition temperature of tetS. $\Delta\Delta G_u^{Tm}$ values are also less accurate than $\Delta\Delta G_u^{[D]50\%}$ values (see text).
[b]Percentage side chain accessibility relative to that in an extended Gly-X-Gly tripeptide; calculated with a 1.7 Å probe and the program MS (Connolly, 1983).

A structural interpretation of the contribution of each side chain to the thermodynamic stability of p53tet

GuHCl denaturation experiments allowed the precise quantitation of the differences in thermodynamic stability between each mutant and wild-type p53tet in the presence of denaturant. However, it is not clear whether linear extrapolation of ΔG_u values to zero denaturant concentration is generally acceptable (Pace, 1986; Johnson and Fersht, 1995), and even less so for oligomeric proteins (Neet and Timm, 1994). GuHCl and urea denaturation of p53tet yielded very similar $\Delta G_u^{H_2O}$ values, which suggests that the linear assumption—as previously seen for the dimeric Arc repressor (Bowie and Sauer, 1989)—is reasonably accurate for tetrameric p53tet. Despite the fact that four (identical) residues were substituted in each p53tet mutant, fairly similar *m*-values were observed for all mutants except those substituted at residue 328 (Table II and unpublished data). The validity of the linear extrapolation and the similarity of the *m*-values led to a good agreement between $\Delta\Delta G_u^{H_2O}$ and $\Delta\Delta G_u^{[D]_{50\%}}$ values, $r = 0.95$).

For p53tetSS, comparison of $\Delta G_D = 23.3$ kcal/mol (Sakamoto *et al.*, 1994) with $\Delta G_u^{H_2O} = 32.4$ kcal/mol (Table I) indicates that each putative folded monomer is stabilized by only 2.4 kcal/mol relative to the denatured state and that quaternary interactions provide about three-quarters of the conformational stability of p53tet (Neet and Timm, 1994). The results obtained here, interpreted in the light of the very simple three-dimensional structure of p53tet, provide a detailed and coherent quantitative picture of the contribution of each side chain to the stability (Figure 8).

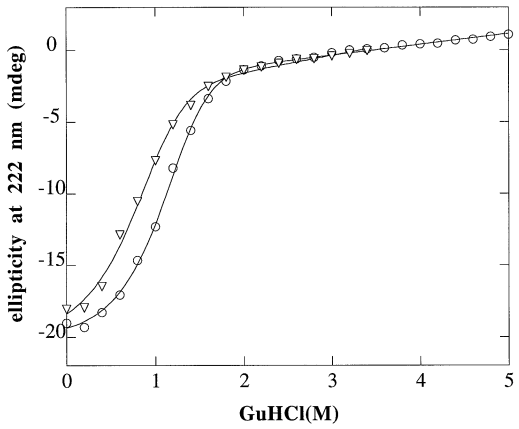

Fig. 7. GuHCl denaturation at 25°C of p53tet dimeric mutants. The fraction of protein denatured for mutants Leu344Ala (○) and Leu348Ala (▽) is represented as a function of GuHCl concentration. The protein (monomer) concentration was 40 μM. The fitting of the experimental values to two-state transition curves (folded dimer–denatured monomer) using the program Kaleidagraph is indicated by solid lines.

The buried residues Leu330, Ile332 and Phe341 make contact with each other at the interface between monomers in each primary dimer and are the most critical for p53tet stability. Thus, they can be considered to form an essential hydrophobic minicore in each dimer (Figure 8). Truncation to Ala of a single buried Leu, Ile or Phe in monomeric

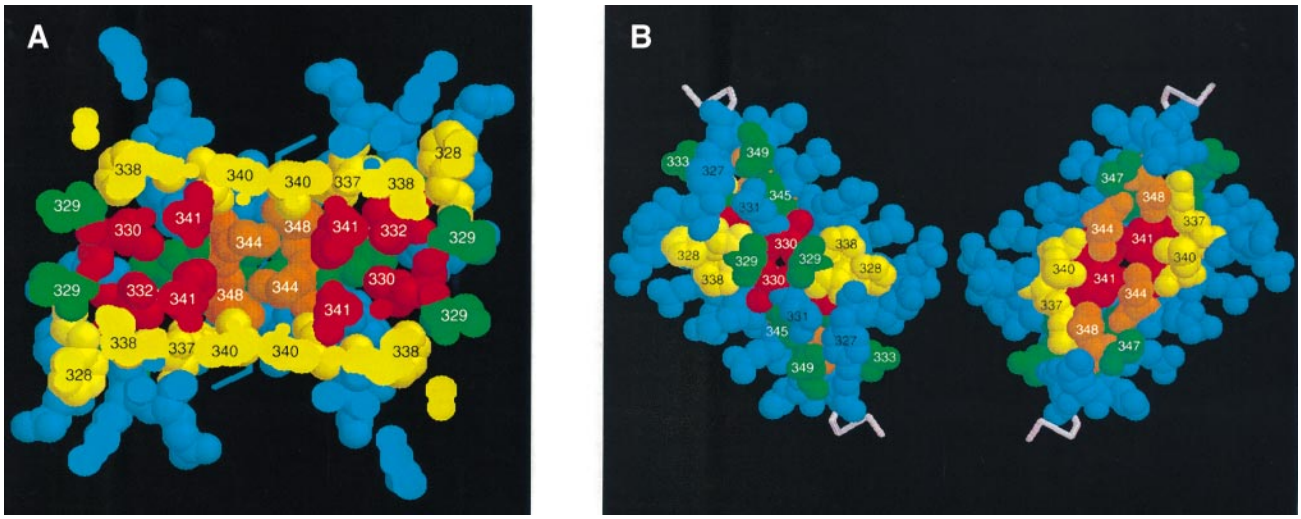

Fig. 8. Effect on p53tet stability of side-chain truncations. Space-filling model of p53tet (residues 326–352; no hydrogens represented) prepared with the program RasMol (Sayle and Milner-White, 1995) and the coordinates used in Figure 1. (**A**) The two primary dimers are depicted on the left and right; the tetramer interface is defined by a vertical plane perpendicular to the image. The proximal half of the model has been removed to allow a direct view of the protein interior. (**B**) The tetramer in (A) was rotated by 90° around the vertical axis and then by 90° around the new axis perpendicular to the image (to obtain the orientation shown in Figure 1), and the two primary dimers were shifted horizontally relative to each other. The tetramer surface and the tetramer interface are thus visible for the dimers on the left and on the right, respectively. The residues are colour-coded according to the effect of their truncation on tet stability: red, extreme destabilization (protein not folded); orange, formation of relatively stable dimers instead of tetramers; yellow, strong destabilization (8.8–11.7 kcal/mol); green, substantial destabilization (4.1–5.7 kcal/mol); blue, no or moderate stabilization or destabilization (–2.1–to 3.9 kcal/mol). Gly334 (no side chain) and the accessible Tyr327 (not tested) are also coloured in blue.

proteins destabilizes the protein from ~2 kcal/mol to 6 kcal/mol and the specific value correlates with the size of the cavity left after any conformational rearrangement (Fersht and Serrano, 1993; Matthews, 1996). The extreme destabilization observed for those p53tet mutants suggests that very large cavities are present in folded Leu330Ala and Phe341Ala. The side chains of Phe328, Phe338, Met340 and the aliphatic portion of Arg337 surround the central minicore and are only partially buried. Accordingly, their truncation caused a less extreme destabilization (Figure 8). The values obtained (2.2–2.9 kcal/mol per side chain) are consistent with studies of monomeric proteins (Fersht and Serrano, 1993; Matthews, 1996; Pace *et al.*, 1996).

Intermonomer polar interactions in each p53tet primary dimer include a surface salt bridge between Arg337 and Asp352 (Clore *et al.*, 1995; Jeffrey *et al.*, 1995), which could provide an alternative explanation for the strong effect of the Arg337 truncation (2.5 kcal/mol per side chain). However, truncation of Asp352 destabilized tet by only 0.7 kcal/mol per side chain. This suggests that the intermonomer salt bridges contribute little to p53tet stabilization and is consistent with the small effect of disrupting intrachain salt bridges in protein surfaces (Fersht and Serrano, 1993). Another intermonomer polar interaction observed is a cluster of water-mediated hydrogen bonds between the backbone amide of Arg333 and both the exposed side chain of Glu349 and the mainly buried side chain of Asn345 (Clore *et al.*, 1995). In monomeric proteins, truncation to Ala of hydrogen-bonded, buried Asn side chains caused a destabilization of ~1–2 kcal/mol (Fersht and Serrano, 1993; Pace *et al.*, 1996). The moderate destabilization of p53tet observed upon truncation of the above-mentioned side chains, in particular Asn345 (1 kcal/mol per side chain) could thus be explained simply by the loss of hydrogen bonds. Truncation of the side chain of Arg333 might affect binding of the water molecule or the local main-chain conformation and prevent hydrogen bond formation. Alternatively, its aliphatic portion could contribute to hydrophobic stabilization. Interestingly, most exposed side chains oriented to solvent were charged, and their individual truncation had some moderate but not insignificant effect on stability in most cases. Truncation of the highly exposed Thr329 destabilized tet by 1.1 kcal/mol per side chain, perhaps because it would partially expose the critical Leu330 to solvent (Figure 8). Overall, the side chains in each monomer appear to contribute to the tertiary and quaternary stabilization of each primary dimer of p53 essentially through hydrophobic interactions and not polar interactions.

The primary dimers in wild-type p53tet are not stable in isolation. Instead, they become stabilized only because of their binary association through the burial of an extended hydrophobic patch. A gradation in the severity of the destabilization caused by truncations at the tetramer interface was observed, depending on the more or less central position of the residue affected (Figure 8). The minor destabilization caused by substitution of the partially accessible Leu350 (0.5 kcal/mol per side chain) was even smaller than expected considering only the partial transfer of the side chains to the protein interior; the location of this residue near the end of the structured domain may facilitate some conformational rearrangement. In contrast, truncation to Gly of the buried Ala347 probably resulted in the formation of two small cavities near the ends of the tetramer interface. The destabilization observed (1.2 kcal/mol per side chain) was close to the average found for the removal of a buried methylene group in monomeric proteins (Green *et al.*, 1992; Fersht and Serrano, 1993). Truncation of the partially buried, centrally

located Met340 was strongly destabilizing but still did not prevent tetramer formation. In contrast to the other side chains, truncation to Ala of either of the two Leu side chains buried at the centre of the tetramer interface (Figure 8) destabilized the tetramer relative to folded dimers. Dimerization of the mutant Leu344Ala was expected because a full-length p53 with this substitution was shown to bind DNA as a dimer (Waterman *et al.*, 1995). Very recently, McCoy *et al.* (1997) extended this result to a few other substitutions of Leu344 (either alone or accompanied by mutation of Phe341). These authors also showed that a triply mutated, isolated tet domain (Leu344Tyr/Phe341Ile/Met340Lys) is effectively a dimer with an altered tertiary structure relative to the dimers in the tetramer. The present study shows that the isolated tetramerization domain is able to form stable dimers instead of tetramers simply by truncation of either of the side chains located centrally at the interface (Leu344 or Leu348), without the need of multiple substitutions or the incorporation of bulky or polar side chains. Our quantitative analysis also revealed that the dimeric tet variants are at the lower end of the stability range for natural dimeric proteins, but that they are reasonably stable for their small size (Neet and Timm, 1994). It is tempting to speculate with possible evolutionary pathways through a single key mutation from functional dimers to tetramers (dimers of dimers) with improved stability or multivalency.

All nine residues critical for p53tet stability were found almost completely conserved among the 11 mammalian p53 genes sequenced (Soussi and May, 1996), while most other tet residues were not. The only exception was the conservative substitution Phe338Tyr detected in two species; modelling of this replacement suggests it would not disrupt any interaction. On the other hand, in human p73—a protein of unknown function with remarkable overall sequence identity to p53 (Kaghad *et al.*, 1997)—Leu344 and Leu348 are conserved, while most other residues critical for p53tet stability (Phe328, Ile332, Arg337, Met340, Phe341 and Ala347) are not. This underscores a special role for those two Leu residues and leads us to suspect that p73 might be a tetramer, although with a hydrophobic core packing different from that of p53.

Comparison with systematic stability studies of other proteins

As discussed above, the results obtained with tetrameric p53tet do not appear to contradict the general principles of protein stability that have emerged from extensive mutational studies of monomeric proteins (e.g. Shortle *et al.*, 1990; Matthews, 1991, 1996; Green *et al.*, 1992; Serrano *et al.*, 1992; Fersht and Serrano, 1993; Otzen *et al.*, 1994). Quantitative determinations of the contribution of each side chain to stability, as described here for tetrameric tet, have been carried out, however, for very few proteins. These include the monomeric BPTI (Yu *et al.*, 1995) and the dimeric Arc repressor (Milla *et al.*, 1994). The results of these latter studies are consistent with the view that nearly half of the side chains in a protein have little or no effect on the stability. In contrast, p53tet appears to be unusually sensitive to mutation. In part, this can be trivially explained by the cumulative effects of the four identical side chains substituted per mutational event. But in addition, even after correction to give $\Delta\Delta G_u$ values per individual side chain, the proportion of neutral or near-neutral alanine substitutions (taken as those with $\Delta\Delta G_u \leqslant 0.3$ kcal/mol per side chain) was found to be only 8% in the 120-residue p53tet compared with ~33% for the 58-residue BPTI (Yu *et al.*, 1995) and 45% for the 106-residue Arc (Milla *et al.*, 1994). In multimeric proteins, the coupling between folding and oligomerization and the symmetry and other structural constraints to be fulfilled on mutation pose interesting evolutionary considerations on the tolerance of amino acid substitutions.

Cancer-associated mutations in p53tet

From the above results it is apparent that some mutations in p53tet may have little effect or lead to reasonably stable, dimeric tet, which could still allow p53 to perform its biological function (Waterman *et al.*, 1995, 1996). However, it is also clear that other single mutational events are able to dramatically shift the equilibrium towards p53 monomers, which would have reduced or no biological activity. These observations, and the reduced DNA-binding activity of some full-length p53 with single mutations in the tet domain (Waterman *et al.*, 1995; Chène *et al.*, 1997), suggest that functional resistance of p53tet to amino acid substitutions may not be the explanation for the remarkable conservation of this domain in tumorigenic processes. Even though point mutations in the tetramerization domain of p53 appear to be very infrequent, mutations in any of at least 12 out of 30 residues within p53tet have been found associated with tumours (Hollstein *et al.*, 1996). The stability results obtained make some of these cancer-associated mutations difficult to rationalize. Those affecting side chains critical for tet stability, like Phe328Leu, Leu330His, Arg337Cys and Leu344Pro, could be predicted to be strongly destabilizing. In addition, Gly334Val might act by distorting the overall conformation (Clore *et al.*, 1995) and Arg342Pro would disrupt the C-terminal helix. However, mutations like Asp326Gly, Gln331His, Glu349Asp, Asp352His might be expected not to have a strongly destabilizing effect. We have confirmed experimentally that, while Phe328Leu is strongly destabilizing, Gln331His has no significant effect on the stability (M.G.Mateu and A.R.Fersht, unpublished data). Some of the p53tet mutations tentatively associated with cancer, if also present in normal cells of the same patient, could instead reflect functionally neutral genetic polymorphisms. Alternatively, some of these mutations might affect some undescribed biological function of the tetramerization domain, perhaps some interaction with other proteins or p53 segments. The residue-by-residue dissection of the thermodynamic stability of the tetramerization domain presented here may also facilitate the engineering of variant p53s with altered hetero-oligomerization properties. We are exploring the introduction of multiple mutations at critical positions of p53tet to achieve a modified oligomerization interface without a negative effect on the thermodynamic stability. Such variants would be unable to hetero-oligomerize with defective p53s from tumour cells and could prove useful in the development of anti-cancer gene therapy.

Materials and methods

DNA cloning and site-directed mutagenesis

p53 tetL, tetS and tetSS (Figure 2) were amplified by the polymerase chain reaction (PCR) method from plasmid pT7-7Hup53 (Midgley *et al.*,

1992). TetL was amplified using oligonucleotides designed to engineer flanking *Nco*I and *Bam*HI restriction sites, and cloned as a fusion protein containing a histidine tail and an enterokinase cleavage site in expression vector pET19b (Novagen). TetS and tetSS were amplified using primers which included *Nde*I and *Bam*HI sites as well as initiation and termination codons immediately flanking the tet sequence, and cloned as unfused proteins in expression vector pET23b+ (Novagen). Recombinant plasmids were obtained from transformed *Escherichia coli* DH5α and purified using the QiaGen miniprep kit, and the inserts sequenced by the dideoxynucleotide method. Mutagenesis of tetS was carried out using the inverse PCR (IPCR) method essentially as described (Hemsley *et al.*, 1989), but using phosphorylated oligonucleotides and the enzyme pfu polymerase (Stratagene). The mutations introduced were confirmed by sequencing the entire coding region and flanking sequences of each mutant.

Protein expression and purification

TetL was expressed in *E.coli* BL21(DE3)pLysS, purified by affinity chromatography in a Ni-NTA–agarose column and cleaved from the histidine tail by enterokinase digestion essentially as described by Johnson *et al.* (1995). TetS (wild-type and all mutants) or tetSS expression was generally carried out in 5×500 ml cultures of *E.coli* BL21(DE3) [or BL21(DE3)pLysS in some instances] grown at 37°C until the OD_{600} reached 1–1.2. The cultures were induced by addition of IPTG to 0.4 mM and further incubated at 37°C for ~3 h. Cells were harvested by centrifugation and kept at –20°C until use. Cell extracts were obtained by sonication in 40 mM MES buffer pH 6, and clarified by centrifugation and filtration through 0.2 μm membranes. The soluble fraction was applied to a SP–Sepharose cation-exchange column (Pharmacia) and the protein was eluted with a 0–0.5 M NaCl gradient in 40 mM MES pH 6 and further purified by size-exclusion FPLC (Superdex 75, Pharmacia) in 40 mM MES pH 6, 200 mM NaCl. Pure p53tet was dialysed against 25 mM sodium phosphate buffer pH 7 using 3000 Da molecular weight cut-off membranes, filtered through 0.2 μm membranes, flash frozen in liquid nitrogen and stored at –70°C. Samples were analysed by SDS–PAGE and Coomassie Blue staining. Tet preparations were judged pure from the absence of detectable contaminating bands in overloaded gels. Recombinant tetS and tetSS were analysed by electrospray mass spectrometry and had the expected molecular mass (±1 Da); the N-terminal methionine was present in ~80% of the molecules. When necessary, purified p53tet solutions were concentrated by ultrafiltration through Centricon-10 membranes (Amicon). Immediately before use, protein aliquots were thawed and filtered through 0.2 μm membranes (Millex-GV4, Millipore) and the protein monomer concentration determined by UV spectrophotometry using the calculated extinction coefficient for monomeric p53tet, $\varepsilon_{280} = 1280\ M^{-1}\cdot cm^{-1}$, corresponding to a single tyrosine (Gill and von Hippel, 1989; Johnson *et al.*, 1995).

Peptide synthesis and purification

30mer p53 synthetic peptides (tetP and variants) were synthesized using an Applied Biosystems peptide synthesizer, deprotected with a mixture of trifluoroacetic acid/phenol/1,2-ethanedithiol/thioanisole following standard procedures, and purified by reverse-phase HPLC in a C8 column (Rainin) using a gradient of 20–60% acetonitrile in water/0.1% trifluoroacetic acid. The purified peptides were lyophilized, dissolved and dialysed against 25 mM sodium phosphate buffer pH 7, and stored and processed as described above for the recombinant proteins.

Analytical size-exclusion chromatography

A calibrated Superdex 75 HR 10/30 FPLC column (Pharmacia) was used. The molecular weight markers and all p53tet samples (40 μM monomer in 200 μl) were eluted at room temperature in 25 mM phosphate buffer pH 7, 200 mM NaCl at 1 ml/min. Solute behaviour was expressed as $K_{av} = (V_e–V_0)/(V_t–V_0)$; V_e, V_0 and V_t correspond respectively to the elution volume of the solute, the void volume and the total volume of the bed.

Differential scanning calorimetry (DSC)

DSC experiments were performed using a Microcal VPDSC. Temperatures from 15 to 110°C were scanned at a rate of 60°C/h. Tet solutions (40–70 μM tetramer in 25 mM phosphate pH 7) were dialysed, filtered and degassed. The dialysis buffer was used for baseline scans. Reversibility was checked by rescanning of the same sample after cooling to the starting temperature.

Fluorescence spectroscopy

A Perkin-Elmer LS5B luminescence spectrometer was used. Tet solutions (40 μM monomer in 25 mM phosphate pH 7 containing 0–6 M GuHCl) were irradiated with UV light (280 nm) and the emission spectra were recorded from 290 to 440 nm. Temperature was kept constant at 25°C and monitored by a thermocouple in the cell.

Circular dichroism (CD) spectroscopy

CD measurements were carried out using a Jasco-720 spectropolarimeter. Far UV–CD spectra were the average of five scans obtained at a rate of 2 nm/min, a response time of 2 s and a bandwidth of 1 nm. Chemical denaturation equilibrium analyses were generally carried out by measuring the ellipticity at 222 nm of tet solutions (40 μM monomer in 25 mM phosphate pH 7) containing different concentrations of GuHCl or urea, using a 1 mm pathlength cell. The temperature was kept constant at 25°C and each sample was allowed to reach chemical and thermal equilibrium. Each ellipticity value was obtained by averaging two time measurements recorded after the signal was stabilized. Thermal denaturation equilibrium analyses were generally carried out using the temperature scan mode and measuring the ellipticity at 222 nm of tet solutions (10 μM monomer in 25 mM phosphate pH 7) in a 5 mm cell. The initial and final temperatures were respectively 2–25°C, and 80–95°C, depending on the mutant analysed. A temperature rate of 50°C/h, a response time of 8 s and a bandwidth of 1 nm were used. The absence of kinetic effects on the data was confirmed by comparing scans performed at a slower rate (10°C/h). Reversibility of the unfolding process was evaluated as for DSC. Temperature was monitored by a thermocouple in the cuvette holder block.

Equilibrium data analysis

Unfolding of p53tet was described as a two-state transition with the native tetramer (N_4; wild-type and most mutants) or dimer (N_2; mutants Leu344Ala and Leu348Ala) directly converted to denatured monomers (U):

$$N_4 \rightleftharpoons 4U \quad \text{or} \quad N_2 \rightleftharpoons 2U$$

The equilibrium constants for tetrameric or dimeric tet unfolding K_u, and the free energy of unfolding ΔG_u are defined as:

$$K_u = [U]^4/[N_4] = 4P_t^3 f_u^4/(1–f_u) \quad (1)\ \text{(tetramer)}$$

$$K_u = [U]^2/[N_2] = 2P_t f_u^2/(1–f_u) \quad (2)\ \text{(dimer)}$$

$$\Delta G_u = –RT \ln K_u \quad (3)$$

P_t is the total p53tet monomer concentration, and f_u the fraction of denatured protein.

Method I: At any given denaturant concentration [D] (chemical denaturation experiments) or temperature T (thermal denaturation), f_u was calculated from the corresponding experimental ellipticity value θ by using the expression (Pace, 1986):

$$f_u = [\theta – (\theta_{n0} + m_n D)]/[(\theta_{u0} + m_u D) – (\theta_{n0} + m_n D)] \quad (4)$$

where D is the [D] or T used. θ_{n0} and θ_{n0}, the ellipticity values corresponding to the native (n) and denatured (u) states extrapolated to $D = 0$, and m_n and m_u, the slopes of the baselines preceding and following the transition region, were obtained by linear regression analysis of the baselines. The low stability of a few mutants precluded a reliable determination of m_n. In such cases, m_n was equated to 0, which was close to the values determined for tetS and most mutants. From equations (1–4),

$$\Delta G_u = –RT \ln\{[4P_t^3(\theta – (\theta_{n0} + m_n D))^4]/ [(\theta_{u0} + m_u D – \theta)(\theta_{u0} – \theta_{n0} + D\,(m_u – m_n))^3]\} \quad (5)\ \text{(tetramer)}$$

$$\Delta G_u = –RT \ln\{[2P_t(\theta – (\theta_{n0} + m_n D))^2]/ [(\theta_{u0} + m_u D – \theta)(\theta_{u0} – \theta_{n0} + D\,(m_u – m_n))]\} \quad (6)\ \text{(dimer)}$$

Chemical denaturation parameters: to calculate $[D]_{50\%}$, $\Delta G_u^{H_2O}$ and m, the ΔG_u values obtained for [D] values within the transition zone of the denaturation curve using equations (5) or (6) were used to fit the appropriate equations:

$$\Delta G_u = \Delta G_u^{H_2O} – m\,[D] \quad (7)$$

$$\Delta G_u = m\,([D]_{50\%} – [D]) – RT \ln(P_t^3/2) \quad (8)\ \text{(tetramer)}$$

$$\Delta G_u = m\,([D]_{50\%} – [D]) – RT \ln P_t \quad (9)\ \text{(dimer)}$$

To minimize errors due to extrapolation, the difference in free energy between any two tetrameric variants (i) and (j), $\Delta\Delta G_{u(ij)}$ was calculated, unless otherwise stated, at a denaturant concentration [D] = $([D]_{50\%}$

(i) – $[D]_{50\%(j)})/2$ (Jackson *et al.*, 1993). *m* was assumed not to change significantly upon single amino acid substitutions (except for mutations of residue 328; see Results), so an average *m*-value, $<m>$, was calculated by averaging the experimental *m*-values obtained for tetS wild-type and all tetrameric mutants except Phe328Ala. Thus,

$$\Delta\Delta G_{u(ij)}^{[D]_{50\%}} = <m> ([D]_{50\%(i)} - [D]_{50\%(j)}) \quad (10)$$

Thermal denaturation parameters: To calculate T_m and ΔH_u^{Tm}, ΔG_u values obtained for *T* values within the transition zone of the denaturation curve using equations (5) or (6) were used to fit the appropriate expanded form of the Gibbs equation:

$$\Delta G_u = \Delta H_u^{Tm} (1 - T/T_m) + \Delta C_p[T - T_m - T \ln(T/T_m)] - RT \ln(P_t^3/2) \quad (11) \text{ (tetramer)}$$

$$\Delta G_u = \Delta H_u^{Tm} (1 - T/T_m) + \Delta C_p[T - T_m - T \ln(T/T_m)] - RT \ln P_t \quad (12) \text{ (dimer)}$$

where ΔC_p = 1.7 kcal/(K.mol of tetramer) or 0.85 kcal/(K.mol of dimer) which correspond to 425 cal/(K.mol of monomer). This value was obtained experimentally for p53tetL by Johnson *et al.* (1995) in very similar conditions and was assumed constant over the relevant temperature range and upon single amino acid mutation. All fittings were performed using the program Kaleidagraph (Abelbeck Software).

Method II: Thermodynamic parameters for chemical and thermal unfolding of tetrameric p53tet were also obtained using the program Excel (Microsoft) by direct non-linear fitting of the experimental ellipticity values in the expression:

$$\theta = (1 - f_u)(\theta_{n0} + m_n D) + f_u(\theta_{n0} + m_u D) \quad (13)$$

which was expanded to express f_u as a function of the relevant thermodynamic parameters. The physically meaningful root of the fourth-order equation $(4P_t^3/K_u)f_u^4 + f_u - 1 = 0$ obtained from (1) was solved:

$$f_u = \{-(s^{1/2}) + [-s + (2/a(s^{1/2}))]^{1/2}\}/2 \quad (14)$$

$$s = -4\{2/[27a + (729a^2 + 6912a^3)^{1/2}]\}^{1/3} + \{1/[3a \{2/[27a + (729a^2 + 6912a^3)^{1/2}]\}^{1/3}]\} \quad (15)$$

$$a = 4P_t^3/\exp(-\Delta G_u/RT) \quad (16)$$

Use of the combined expressions (13–16) and (7), (8) or (11) directly gave the best fitting values for ΔG_u^{H2O} or $[D]_{50\%}$, *m*, θ_{n0}, m_n, θ_{u0} and m_u, or T_m, ΔH_u^{Tm}, θ_{n0}, m_n, θ_{u0} and m_u.

Thermodynamic parameters for chemical and thermal unfolding of dimeric p53tet were also obtained using the program Kaleidagraph by direct non-linear fitting of the experimental ellipticity values in the expression (Mok *et al.*, 1996):

$$\theta = (\theta_{n0} + m_n D) - \{[(\theta_{n0} + m_n D) - (\theta_{u0} + m_u D)] [\exp(-\Delta G_u/RT)][(1 + 8P_t/\exp(-\Delta G_u/RT))^{1/2} - 1]/4P_t\} \quad (17)$$

Use of the combined expressions (17) and (7), (9) or (12) directly gave the best fitting values for the relevant parameters. When the values of the thermodynamic parameters obtained with methods I and II were compared small, non-significant differences were generally observed. This was mainly due to the assumptions of each method concerning the baselines before and after the transition region. Unless otherwise stated, the values and the corresponding standard errors of fitting obtained using method I are given.

Acknowledgements

We gratefully acknowledge Drs M.Bycroft, C.Johnson, J.L.Neira and M.S.del Pino and M.Proctor, for expert advice on different techniques and for scientific discussions, Prof. D.Lane for the gift of plasmid pT7-7Hup53 and for discussions, Dr N.Verdaguer for solvent accessibility calculations, and K.von Glos for peptide synthesis. This work was supported by the CRC of the UK. M.G.M. was supported by grants from the Ministerio de Educación y Ciencia of Spain (until October 1997) and the European Union (from November 1997).

References

Arrowsmith,C.H. and Morin,P. (1996) New insights into p53 function from structural studies. *Oncogene*, **12**, 1379–1385.

Beaudry,G.A., Bertelsen,A.H. and Sherman,M.I. (1996) Therapeutic targeting of the p53 tumor suppressor gene. *Curr. Opin. Biotechnol.*, **7**, 592–600.

Bowie,J.U. and Sauer,R.T. (1989) Equilibrium dissociation and unfolding of the Arc repressor dimer. *Biochemistry*, **28**, 7139–7143.

Chène,P., Mittl,P. and Grütter,M. (1997) In vitro structure-function analysis of the β-strand 326–333 of human p53. *J. Mol. Biol.*, **273**, 873–881.

Clore,G.M., Omichinski,J.G., Sakaguchi,K., Zambrano,N., Sakamoto,H., Appella,E. and Gronenborg,A. (1994) High-resolution structure of the oligomerization domain of p53 by multidimensional NMR. *Science*, **265**, 386–391. [Correction in *Science*, **267**, 1515–1516 (1995).]

Clore,G.M., Ernst,J., Clubb,R., Omichinski,J.G., Kennedy,W.M.P., Sakaguchi,K., Appella,E. and Gronenborg,A. (1995) Refined solution structure of the oligomerization domain of the tumour suppressor p53. *Nature Struct. Biol.*, **2**, 321–333.

Connolly,M.L. (1983) Analytical molecular surface calculation. *J. Appl. Crystallogr.*, **16**, 548–558.

El-Deiry,W.S., Kern,S.E., Pietenpol,J.A., Kizler,K.W. and Vogelstein,B. (1992) Definition of a consensus binding site for p53. *Nature Genet.*, **1**, 45–49.

Fersht,A.R. and Serrano,L. (1993) Principles of protein stability derived from protein engineering experiments. *Curr. Opin. Struct. Biol.*, **3**, 75–83.

Gill,S.C. and von Hippel,P.H. (1989) Calculation of protein extinction coefficients from amino acid sequence data. *Anal. Biochem.*, **182**, 319–326.

Green,S.M., Meeker,A.K. and Shortle,D. (1992) Contributions of the polar, uncharged amino acids to the stability of staphylococcal nuclease: evidence for mutational effects on the free energy of the denatured state. *Biochemistry*, **31**, 5717–5728.

Hann,B.C. and Lane,D.P. (1995) The dominating effect of mutant p53. *Nature Genet.*, **9**, 221–222.

Harvey,M., Vogel,H., Morris,D., Bradley,A., Bernstein,A. and Donehower,L.A. (1995) A mutant p53 transgene accelerates tumor-development in heterozygous but not nullizygous p53 deficient mice. *Nature Genet.*, **9**, 305–311.

Hemsley,A., Arnheim,N., Toney,M.D., Cortopassi,G. and Galas,D.J. (1989) A simple method for site-directed mutagenesis using the polymerase chain reaction. *Nucleic Acids Res.*, **17**, 6545–6551.

Hollstein,M., Sidransy,D., Vogelstein,B. and Harris,C.C. (1991) p53 mutations in human cancers. *Science*, **253**, 49–53.

Hollstein,M., Shimer,B., Greenblatt,M., Soussi,T., Hovig,E., Montesano,R. and Harris,C.C. (1996) Somatic point mutations in the p53 gene of human tumors and cell lines: updated compilation. *Nucleic Acids Res.*, **24**, 141–146.

Ishioka,C., Englert,C., Winge,P., Yan,Y.-X., Engelstein,M. and Friend,S. (1995) Mutational analysis of the carboxy-terminal portion of p53 using both yeast and mammalian cell assays *in vivo*. *Oncogene*, **10**, 1485–1492.

Jackson,S.E., Moracci,M., el Masry,N., Johnson,C.M. and Fersht,A.R. (1993) Effect of cavity-creating mutations in the hydrophobic core of chymotrypsin inhibitor 2. *Biochemistry*, **32**, 11259–11269.

Jeffrey,P.D., Gorina,S. and Pavletich,N.P. (1995) Crystal structure of the tetramerization domain of the p53 tumor suppressor at 1.7 Angstroms. *Science*, **267**, 1498–1502.

Johnson,C.M. and Fersht,A.R. (1995) Protein stability as a function of denaturant concentration: the thermal stability of barnase in the presence of urea. *Biochemistry*, **34**, 6795–6804.

Johnson,C.M., Oliveberg,M., Clarke,J. and Fersht,A.R. (1997) Thermodynamics of denaturation of mutants of barnase with disulfide crosslinks. *J. Mol. Biol.*, **268**, 198–208.

Johnson,C.R., Morin,P.E., Arrowsmith,C.H. and Freire,E. (1995) Thermodynamic analysis of the structural stability of the tetrameric oligomerization domain of p53 tumor suppressor. *Biochemistry*, **34**, 5309–5316.

Kaghad,M. *et al.* (1997) Monoallelically expressed gene related to p53 at 1p36, a region frequently deleted in neuroblastoma and other human cancers. *Cell*, **90**, 809–819.

Ko,L.J. and Prives,C. (1996) p53: puzzle and paradigm. *Genes Dev.*, **10**, 1054–1072.

Kraulis,P.J. (1991) Molscript. a program to produce both detailed and schematic plots of protein structures. *J. Appl. Crystallogr.*, **24**, 946–950.

Lee,W., Harvey,T.S., Yin,Y., Yau,P., Litchfield,D. and Arrowsmith,C.H. (1994) Solution structure of the tetrameric minimum transforming domain of p53. *Nature Struct. Biol.*, **1**, 877–890.

Levine,A.J. (1997) p53, the cellular gatekeeper for growth and division. *Cell*, **88**, 323–331.

Matthews,B.W. (1991) Studies on protein stability with T4 lysozyme. *Adv. Protein Chem.*, **46**, 249–278.

Matthews,B.W. (1996) Structural and genetic analysis of the folding and function of T4 lysozyme. *FASEB J.*, **10**, 35–41.

McCoy,M., Stavridi,E.S., Waterman,J.L.F., Wieczorek,A.M., Opella,S.J. and Halazonetis,T.D. (1997) Hydrophobic side-chain size is a determinant of the three-dimensional structure of the p53 oligomerization domain. *EMBO J.*, **16**, 6230–6236.

Midgley,C.A., Fischer,C.J., Bartek,J., Vojtesek,B., Lane,D. and Barnes,D. (1992) Analysis of p53 expression in human tumours: an antibody raised against human p53 expressed in *Escherichia coli*. *J. Cell Sci.*, **101**, 183–189.

Milla,M.E., Brown,B.M. and Sauer,R.T. (1994) Protein stability effects of a complete set of alanine substitutions in Arc repressor. *Nature Struct. Biol.*, **1**, 518–523.

Miller,M. *et al.* (1996) The oligomerization domain of p53: crystal structure of the trigonal form. *FEBS Lett.*, **399**, 166–170.

Mok,Y.-K., De Prat Gay,G., Butler,P.J. and Bycroft,M. (1996) Equilibrium dissociation and unfolding of the dimeric human papillomavirus strain-16 E2 DNA-binding domain. *Protein Sci.*, **5**, 310–319.

Neet,K.E. and Timm,D.E. (1994) Conformational stability of dimeric proteins: quantitative studies by equilibrium denaturation. *Protein Sci.*, **3**, 2167–2174.

Otzen,D.E., Itzhaki,L.S., el Masry,N.F., Jackson,S.E. and Fersht,A.R. (1994) Structure of the transition state for the folding/unfolding of the barley chymotrypsin inhibitor-2 and its implications for mechanisms of protein folding. *Proc. Natl Acad. Sci. USA*, **91**, 10422–10425.

Pace,C.N. (1986) Determination and analysis of urea and guanidine hydrochloride denaturation curves. *Methods Enzymol.*, **131**, 266–280.

Pace,C.N., Shirley,B.A., McNutt,M. and Gajiwala,K. (1996) Forces contributing to the conformational stability of proteins. *FASEB J.*, **10**, 75–83.

Pavletich,N., Chambers,K.A. and Pabo,C.O. (1993) The DNA-binding domain of p53 contains the four conserved regions and the major mutation hot spots. *Genes Dev.*, **7**, 2556–2564.

Picksley,S.M. and Lane,D.P. (1994) p53 and Rb: their cellular roles. *Curr. Opin. Cell Biol.*, **6**, 853–858.

Sakaguchi,K., Sakamoto,H., Lewis,M.S., Anderson,C.W., Erickson,J.W., Appella,E. and Xie,D. (1997) Phosphorylation of serine 392 stabilizes the tetramer formation of tumor suppressor protein p53. *Biochemistry*, **36**, 10117–10124.

Sakamoto,H., Lewis,M.S., Kodama,H., Appella,E. and Sakaguchi,K. (1994) Specific sequences from the carboxyl terminus of human p53 gene product form anti-parallel tetramers in solution. *Proc. Natl Acad. Sci. USA*, **91**, 8974–8978.

Sayle,R.A. and Milner-White,E.J. (1995) RasMol: biomolecular graphics for all. *Trends Biochem. Sci.*, **20**, 374–376.

Serrano,L., Kellis,J.T.,Jr, Cann,P., Matouschek,A. and Fersht,A.R. (1992) The folding of an enzyme. II. Substructure of barnase and the contribution of different interactions to protein stability. *J. Mol. Biol.*, **224**, 783–804.

Shaulian,E., Zauberman,A., Ginsberg,D. and Oren,M. (1992) Identification of a minimal transforming domain of p53: negative dominance through abrogation of sequence-specific DNA binding. *Mol. Cell. Biol.*, **12**, 5581–5592.

Shortle,D., Stites,W.E. and Meeker,A.K. (1990) Contributions of the large hydrophobic amino acids to the stability of staphylococcal nuclease. *Biochemistry*, **29**, 8033–8041.

Soussi,T. and May,P. (1996) Structural aspects of the p53 protein in relation to gene evolution: a second look. *J. Mol. Biol.*, **260**, 623–637.

Stürzbecher,H.-W., Brain,R., Addison,C., Rudge,K., Remm,M., Grimaldi,M., Keenan,E. and Jenkins,J.R. (1992) A C-terminal α-helix plus basic region motif is the major structural determinant of p53 tetramerization. *Oncogene*, **7**, 1513–1523.

Wang,P., Reed,M., Wang,Y., Mayr,G., Stenger,J., Anderson,M.E., Schwedes,J.F. and Tegtmeyer,P. (1994) p53 domains: structure, oligomerization and transformation. *Mol. Cell. Biol.*, **14**, 5182–5191.

Waterman,J.L.F., Shenk,J.L. and Halazonetis,T.D. (1995) The dihedral symmetry of the p53 tetramerization domain mandates a conformational switch upon DNA binding. *EMBO J.*, **14**, 512–519.

Waterman,M.J.F., Waterman,J.L.F. and Halazonetis,T.D. (1996) An engineered four-stranded coiled-coil substitutes for the tetramerization domain of wild-type p53 and alleviates transdominant inhibition by tumor-derived p53 mutants. *Cancer Res.*, **56**, 158–163.

Yu,M.-H., Weissman,J.S. and Kim,P.S. (1995) Contribution of individual side chains to the stability of BPTI examined by alanine-scanning mutagenesis. *J. Mol. Biol.*, **249**, 388–397.

Received January 28, 1998; revised March 13, 1998; accepted March 16, 1998